Melting of Pb clusters without free surfaces

Z. H. Jin,* H. W. Sheng, and K. Lu
State Key Lab for Rapidly Solidified Non-equilibrium Alloys, Institute of Metal Research, Chinese Academy of Sciences, Shenyang 110015, People's Republic of China

(Received 14 April 1998; revised manuscript received 13 October 1998)

Melting behaviors of Pb clusters without free surfaces have been studied using molecular dynamics and the Sutton-Chen (SC) potential. Two Pb clusters (Pb^N, with $N=201$ and 249) are selected and each of them has been embedded in the core of an Al^{4033} cubo-octahedron, but with different orientation relationship with Al coatings. For the Pb^{201} cluster, where a parallel cube-cube relationship exists with the Al lattice, semicoherent interfaces can be formed and the core can be superheated up to 750 K, in comparing to the equilibrium melting point of 615 ± 10 K for bulk Pb predicted using the SC potential. On further elevating the temperature, a simultaneous melting of both the Pb core and the outer Al coating will occur. For the Pb^{249} cluster without a parallel orientation relationship with Al, no effective semicoherent interface can be formed, and the core premelts at about 500 K without breaking the crystalline structure of Al shells. The melting point of the Pb inclusions can be predicted using thermodynamic relations. For different Pb-Al interfaces, two melting mechanisms exist: one is the homogeneous melting which leads to a melting point elevation and the other is the heterogeneous melting which can induce a melting point depression. [S0163-1829(99)09625-3]

I. INTRODUCTION

In recent years there has been an increased interest in investigating the melting behaviors of nanometer-sized metallic clusters.[1] A comprehensive understanding of the melting phenomenon is crucial because it is directly related to the stability, structure and size of the clusters. It is well known that the melting point (T_m) of a small cluster with free surface, i.e., an isolated cluster in vacuum, is lower than that of the infinite bulk solid.[2] This can be understood according to phenomenological models by emphasizing the enhanced surface effects due to the small size. When the particle size is decreased, its surface to volume ratio increases, and T_m decreases as a consequence of the improved free energy at the cluster surface.[3,4]

On the other hand, in the absence of free surface, many pieces of evidence suggest that encapsulating crystallites within higher-melting-point host matrices can achieve superheating or, melting point elevation. Silver clusters with gold coating can be superheated up to 25 K above silver's melting point.[5] Inclusions of Pb in an Al matrix with sizes ranging from 1 nm to 20 nm melt in the temperature range from 603 K to about 673 K.[6–8] And Ar bubbles injected into Al lattice remains to be crystalline up to a temperature of 730 K, i.e., almost two times higher than T_m of the bulk solid.[9] It was shown that the superheating could not be explained alone by the pressure increase from the volume expansion on melting.[6] Instead, under these circumstances, the role of the solid-solid interfaces is emphasized and melting can be hindered by the depressed mean square amplitude of vibration of atoms at the interfaces.[10]

It was also reported that, in analogy with the melting point depression of free clusters, the change in T_m of the superheated clusters is size dependent and proportional to the inverse size of the embedded clusters,[6,8] underlying that the smaller the cluster, the higher the T_m. But the size effect is no longer the single factor to account for the superheating. Studies performed on Pb aggregates in SiO demonstrated that instead of superheating, the T_m was reduced relative to the bulk.[11] While the superheating of lead crystallites on a carbon surface will depend on both size and shape.[12] Our recent results for the ''as-quenched'' and ''as-milled'' samples of Pb particles embedded in Al matrix also indicate that in order to achieve superheating, coherent or semicoherent interface must be formed.[13] In fact, a form of a crystalline solid in epitaxy relationship with the matrix solid is inevitably observed in almost all the circumstances of the superheated clusters,[6–9,14] which can lead significant superheating of the interior clusters by effectively eliminating the possible heterogeneous nucleation sites. However, due to a broad range of size distribution and the transient nature of the melting process, difficulties arise when studying the possible melting mechanisms experimentally, which has hindered further explorations of the structural transitions, the energetic characteristics of clusters and the kinetics of the various melting processes. This makes computer simulation methods, and in particular, molecular dynamics (MD), an excellent tool for investigating the melting phenomenon.

Although the number of MD studies of melting property and structural stability for free clusters and surfaces appear to be enormous,[4,15–29] simulations for the superheated metallic clusters have been rarely reported. What merits mentioned is a MD study of the superheating behavior of coated Lennard-Jones clusters.[30] It demonstrated that the degree of superheating would depend upon both the thickness of the coatings and the differing strength of the interaction between the core and the outer material. The melting transition was predicted to be first-order-like and the cluster melts from the surface inwards. The core cluster will not melt until the disordering of the coating atoms destroys the epitaxy interface. However, no further simulations were carried out for theoretical understandings of the intrinsic differences of melting mechanisms for clusters with and without constraints.

In regard to the melting origin, it still remains a much

debated subject,[10,31] due to the fact that different structures may have different melting mechanisms and several mechanisms may even operate simultaneously.[32] However, it is more convenient for us to recognize that melting can be initiated by two distinct mechanisms.[24,33–36] First, for systems with extrinsic defects such as free surfaces, grain boundaries and voids, the process can be referred as heterogeneous melting since these defects act as the heterogeneous nucleation sites. And second, by contrast, for systems without extrinsic defects, or there is no effective heterogeneous nucleation site for the liquid phase, melting is an intrinsic process initiated by a spontaneous homogeneous nucleation mechanism. A homogeneous melting can lead to a higher melting point beyond that of the bulk solid and this has been studied in details for a surface-free bulk Al crystal[35] as well as confined thin films.[37]

In this paper, the melting behaviors of Pb clusters with Al coatings have been studied using molecular dynamics and the Sutton-Chen (SC) many-body interatomic potentials.[38] In Sec. II, we determine the T_ms for the bulk solid, some low index surfaces and free clusters of Pb. In Sec. III, we present results for melting of two Pb clusters with Al coatings. The discussions are given in Sec. IV and the conclusions are drawn in Sec. V.

II. MELTING POINTS OF BULK SOLID, LOW-INDEX SURFACES AND FREE CLUSTERS OF Pb

The T_ms of the bulk Pb crystal, some low-index surfaces and clusters with free surfaces have been determined using molecular dynamics. The accuracy of the SC potential can be tested and some essential properties can be known for further studies of the coated clusters.

First, the equilibrium melting point (T_0) of Pb solid was estimated by applying the method formerly described by Ercolessi *et al.*[39] For a system where the solid and liquid phase are simultaneously present and in contact, the T_0 can be determined by achieving the coexistence conditions, i.e., lack of motion of the solid-liquid (SL) interface. With samples of different orientations of a Pb crystal [e.g., along (111) and (110) directions], the calculated T_0 value was found to be 615 ± 10 K, which is in reasonable agreement with the experimental value $T_0^{\exp}=600.7$ K. It should be noted that for a MD box containing only the crystalline arrays of atoms bounded with periodic boundary conditions, the melting point is found to be as high as 725 ± 5 K. This happens because no heterogeneous nucleation site, such as free surface or SL interface, can present. This melting point, also known as the intrinsic mechanical melting point T_m^i, can be related to a homogeneous melting mechanism and used for an understanding of the melting behavior of embedded clusters.[37]

Second, surface melting has been examined separately by simulating some low-index surfaces of Pb thin films. In doing this, we have constructed several thin-film crystals with only x-y periodic boundary conditions. This creates double free surfaces perpendicular to the z axis. If the slab is thick enough, the interactions between the two free surfaces can be neglected and each free surface can represent a flat free surface of a bulk solid. The melting process of three low-index surfaces, i.e., (110), (100), and (111), were simulated using the constant-volume and constant-temperature MD program.

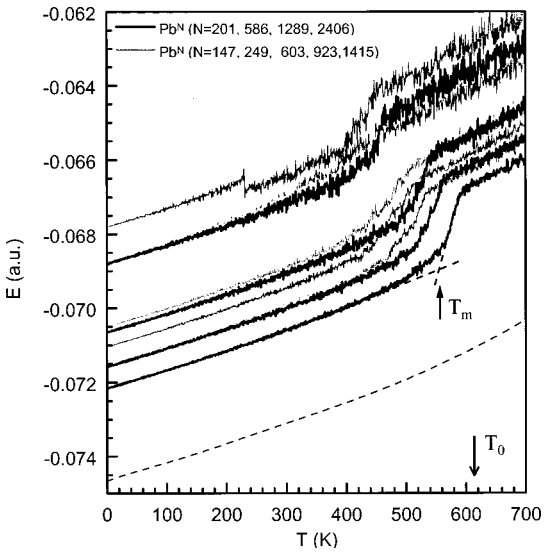

FIG. 1. Variations of potential energy (E) with temperature for melting of free Pb clusters. Thin lines (from top to bottom) represents the E-T curves of Pb^{147}, Pb^{249}, Pb^{603}, Pb^{923}, and Pb^{1415}. Thick lines (from top to bottom) represent the E-T curves of Pb^{201}, Pb^{586}, Pb^{1289}, and Pb^{2406}. For Pb^{147}, a transition from a cubo-octahedral cluster to a icosahedral cluster has been detected. T_0 is the equilibrium melting point for bulk Pb solid. Also shown is the procedure in determining the melting point of a cluster such as in the case of Pb^{2406}.

Our results indicated that the (110) surface melted below 600 K, the (100) surface at slightly above 610 K and the (111) surface at 640 K. The premelting, incomplete melting, and overheating phenomena for the three surfaces, respectively, are in agreement with experimental observations and other MD simulations results.[16–26,40] Further, the melting is initiated at the free surface and then propagates inwards, and the role of free surfaces as providing heterogeneous nucleation sites can be well recognized. For Al, similar results can be obtained for the SC potential and the melting of the simulated low-index surfaces occurs below 970 K.

Third, melting of Pb clusters with free surface has been simulated. A number of Pb clusters, i.e., Pb^{201}, Pb^{586}, Pb^{1289}, Pb^{2406}, and Pb^{4033} in the tronco-octahedral geometry, Pb^{147}, Pb^{561}, Pb^{923}, and Pb^{1415} in the cubo-octahedral geometry, and Pb^{249} and Pb^{603} which are ''spherical'' clusters, have been chosen for the melting studies. All these clusters are bounded with (100) and (111) planes except for the ''spherical'' clusters where other facets such as (110) exhibit. Melting behaviors of clusters will depend on both size and shape. Figure 1 shows the temperature dependence of the average potential energy per atom for our simulated clusters. The melting transition is clearly identifiable by a large upward jump in energy with a finite slop. This occurs because melting first occurs at the vertices and edges, and after the outer shells of the clusters became into a liquid layer, melting of the whole clusters started from the liquid layer to core region very quickly. For clarity, the melting point for a cluster is defined as the intersection of the extrapolated E-T curves from both the low temperature end and the high temperature end around the melting transition (see Fig. 1 for Pb^{2406}). The characteristics of the melting of clusters can be summarized as following.

For cubo-octahedral clusters such as Pb^{147}, transformations to icosahedronlike clusters before melting will occur. This suggests that, in the Sutton-Chen scheme, a small icosahedral cluster can be more stable than a fcc cubo-octahedral cluster of the same size. The reason for this should be attributed to that the SC potentials are simple power law potentials as well as they are fitted using parameters for bulk solids. Our MD studies show that the transition from a bulk-like structure to a structure with fivefold symmetry only occurs when clusters containing less than 1000 atoms for metals such as Pb and Al.

For spherical-like clusters, the situation is even more complex. Since these clusters show not only (100) and (111), but also (110) or other relatively unstable facets, they appears to be less stable than other clusters we simulated. As the temperature is increased, these clusters will readjust their shape in order to find the minimum-energy configuration. And this has led more significant fluctuations in the E-T curves before complete melting of these clusters.

The tronco-octahedral cluster appears to be most stable. The relation between the size and the melting temperature $T_m(R)$ can be predicted using a simple thermodynamic theory[3] based solely on equating the Gibbs free energies of solid and liquid clusters, in assuming that the clusters are spherical particles of radius R, i.e.,

$$\frac{T_0 - T_m(R)}{T_0} = \frac{2}{\rho_s L R}\left[\gamma_{\mathrm{SV}} - \left(\frac{\rho_s}{\rho_l}\right)^{2/3}\gamma_{\mathrm{LV}}\right], \tag{1}$$

where T_0 is the equilibrium melting temperature of bulk solid, ρ is the density, L is the latent heat on melting, and γ_{SV} and γ_{LV} are the solid-vapor and liquid-vapor interfacial energies, respectively. Furthermore, such a relation can be converted into

$$T_m(N) = T_0(\infty) - AN^{-1/3}, \tag{2}$$

where N is the number of the atoms involved in the particle and A is a constant. The best fit of the MD data (Fig. 2) yields $T_0(\infty) = 612.0\,\mathrm{K}$ and $A = -1.01\times 10^3\,\mathrm{K}$. The $T_0(\infty)$ value is very close to that predicted for the bulk solid, demonstrated again that the SC potential is quite adequate in reproducing the bulk melting properties of Pb. For T_m's of other clusters, it is shown in Fig. 2 that there is a strong dependence on both size and shape.[41]

III. MELTING OF THE COATED Pb CLUSTERS

Melting processes of Pb clusters without free surfaces were simulated. Two small free clusters with different size and shape, i.e., $Pb^{201}(A)$ and $Pb^{249}(B)$, were chosen and each of them has been embedded into the core of a much larger tronco-octahedral Al^{4033} cluster. In embedding a Pb cluster in Al, the nearest neighbor distance between Pb and Al atoms is set to be $r_{\text{Pb-Al}} \geqslant 3.33\,\text{Å}$. This value was obtained by evaluating the first peak position of the partial pair distribution functions for the unlike pairs calculated for the MD simulated $Al_{50}Pb_{50}$ liquid. It is always found to be larger than the mean values of the nearest neighbor distances for the like pairs, i.e., Pb-Pb and Al-Al, because of the existence of a strong phase separation tendency in the system. In doing this, we can obtain fully relaxed interfaces by eliminating extra interfacial stresses due to the lattice mismatch induced by different thermal expansions for the two metals.[42]

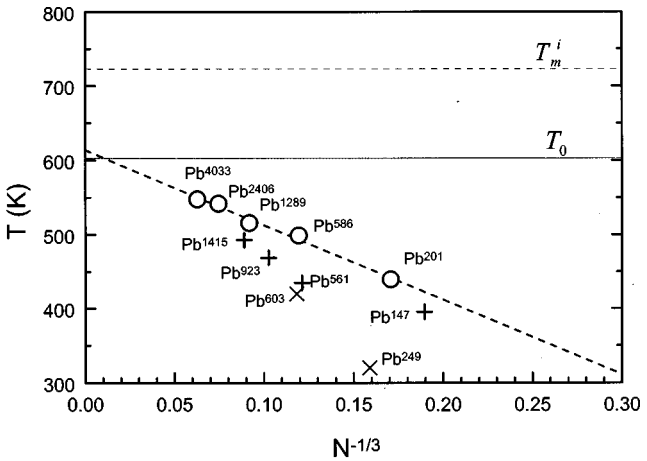

FIG. 2. Melting points vs $N^{1/3}$ for Pb^N clusters. For tronco-octahedral clusters, a linear relation has been fitted according to Eq. (2). The experimentally measured melting point (T_0) for bulk Pb and the intrinsic melting point (T_0^i) of a MD simulated surface-free Pb crystal (a 500-atom system with periodic boundary conditions) are also shown for comparisons.

One significant difference between the two model clusters is that the two Pb cores is in different orientational relationships with the outer Al coatings, as shown schematically in Fig. 3. For cluster A, the core Pb^{201} cluster is in a parallel cube-cube relationship with the Al coating, i.e., $[001]_{\mathrm{Pb}}\|[001]_{\mathrm{Al}}$, and $[111]_{\mathrm{Pb}}\|[111]_{\mathrm{Al}}$. For cluster B, the core Pb^{249} cluster has been rotated around the [100] direction for about 50° before embedding it into Al, hence, no cube-cube relationship of cluster A exists in cluster B except for two small (100) facets. The two clusters is used to represent two typical structures observed experimentally, i.e., cluster A is for sample prepared by melt-spun[13,43] or ion-implantation[6] while cluster B is for the ball milled sample.[13] It should be noted that the size of our sample might be too small and hence too difficult to be observed experimentally. However, they are convenient in saving computer time and sufficient enough to reveal the underlying basic physics of the melting of the confined particles. Furthermore, free clusters Pb^{201} and Pb^{249} show almost equal average potential energy per atom before melting, makes it rather easy to evaluate the strength of constraints due to different orientational relationships with the Al coating. The total number of the atoms in cluster A and B are 3655 and 3579, respectively, indicating that there should be more point defects (vacancies) in the initial input structure of cluster B.

The main part of our MD simulation has been performed similarly to the cases as presented in Sec. II. The time step is set to be $\Delta t = 5.0\times 10^{-15}\,\mathrm{s}$ and the velocities of the particles are rescaled using the Verlet velocity algorithm. Before heating we relaxed the system by running a 50 000 MD time steps at low temperatures, allowing unfavorable configurations in the interfaces to be relaxed, and then the temperature was elevated at a heating rate of $10^{12}\,\mathrm{K/s}$.

A. Superheating

The response of the mean average potential energy (E) to temperature (T) for the Pb core and Al coating are shown in

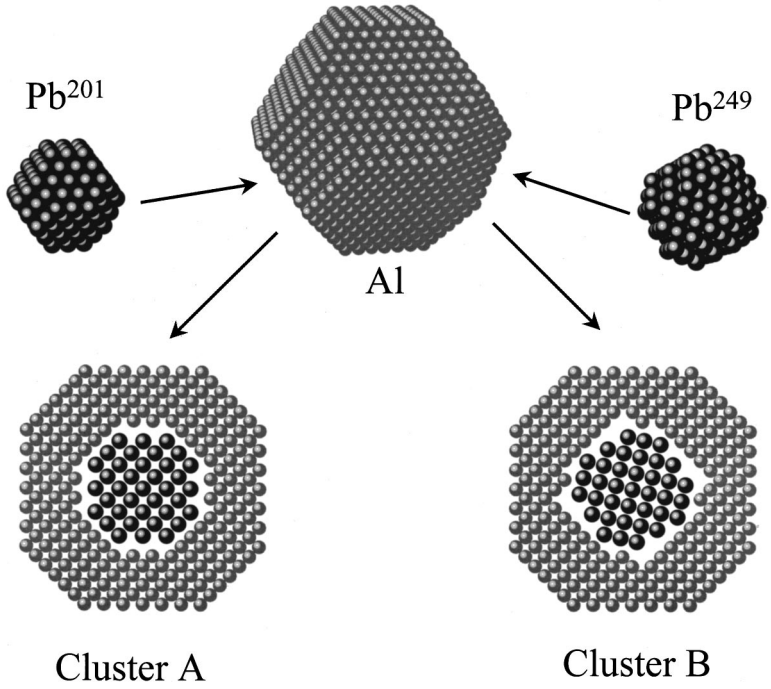

FIG. 3. A schematic illustration of the constructions of the two embedded Pb clusters with Al coatings (cluster *A* and *B*) investigated in MD simulations.

Figs. 4(a) and 4(b), respectively. It is found that cluster *A* can be superheated up to 140 K beyond the equilibrium melting point T_0 of bulk solid. First, there is a small upward jump for Pb and a decrease for Al coating in the low temperature region ($100 \sim 150$ K, denoted as T_r). Then, following the heating of the system to 700 K, the variations of *E* with *T* for both Pb and Al are in a linear manner and almost identical slopes. Finally, at about 730 K, a sudden upward change occurs for both the core and the coating, indicating a dominating structural transition has occurred for the whole system. To identify the two structural transitions, we have recorded configurations of the system at different temperatures. Careful examinations indicate that the system first undergoes a structural reconstruction at the Al-Pb grain boundaries and this process has resulted not only a fully relaxed stable interface but also some degree of coherency between the crystalline lattices of the confined Pb cluster and the Al coating. From the section views of the cluster *A* at different temperatures, as illustrated in Fig. 5(a), we can see that the interfaces have become more relaxed in comparing with the initial input structure as shown in Fig. 3. And after the structural reconstruction, semicoherent interfaces can be formed. At the same time, a few dislocations have been generated from the grain boundaries due to the large lattice misfit effect, passing through the coating lattice of Al and ending at the cluster surface (see also Fig. 6).

The observed reconstruction mode was not detected in experiments to the authors' present knowledge, possibly due to the transient nature of the relaxation process for real materials. In comparing with the experimental observations,[6,8,13,14] the formation of dislocations may be associated with the appearance of the free surface of Al coating. Also, the thickness of the Al coating in MD sample may be much smaller than that of the matrix substance between two nearby Pb inclusions in experimentally obtained Pb-Al samples. Nevertheless, our result is informative because it elucidates a possible way of the formation of semicoherent interfaces.

Whence a semicoherent condition in the interfacial region has been reached, the thermal stability of confined Pb par-

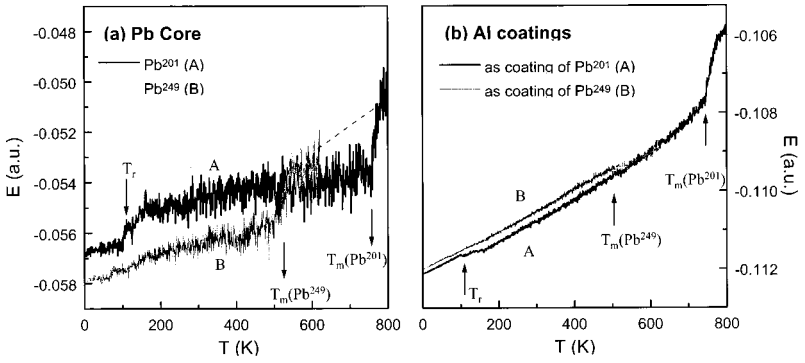

FIG. 4. Melting curves of two Pb clusters with Al coatings obtained by MD simulations.

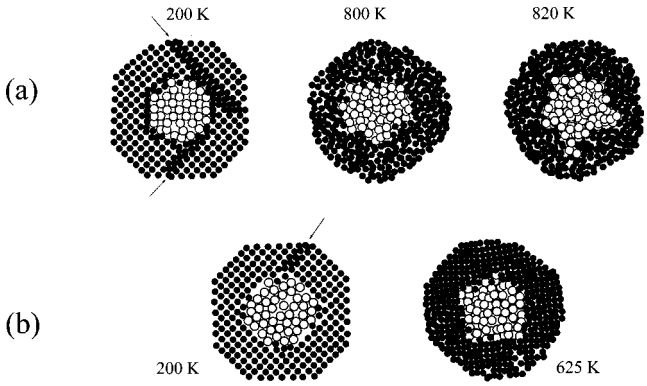

FIG. 5. Cross-section views of the atomic coordination of two coated clusters at different temperatures (open circle is Pb, full circle is Al, and arrows indicate some dislocations generated after MD relaxations): (a) cluster *A*; (b) cluster *B*.

ticle can be strengthened. Two different mechanisms can be proposed for the combined melting of the core and coating of cluster *A*. First, melting is initiated at the free surface of the entire cluster, as in the case of free clusters consisting of only one component. Whence the surface epitaxy relationship with the coating materials is destroyed, melting of the core can take place. Second, the melting of the Pb core leads to the melting of the whole cluster, by destroying the epitaxy Al-Pb interfaces from the inside. It seems that the first mechanism can be ruled out because further simulation indicates the melting point of the free-surface Al^{4033} cluster is above 800 K. Though the Al coating of cluster *A* contains defects due to the generation of dislocations, it is still thick enough to be in a solid state below 800 K. So the second mechanism, i.e., melting is induced by the instability of the core cluster, appears to be the acceptable. That is, for this case, the melting point of the whole cluster is mainly controlled by the maximum degree of the superheating of the Pb clusters without free surfaces.

After the whole cluster has transformed into a liquid state, the shape of the cluster *A* tends to be spherical-like (some flat facets are also observable due to thermal fluctuations; see also Ref. 44). As the temperature is further elevated, there is a tendency for Pb atoms to escape from the core of the cluster as shown in Fig. 5(a) (cluster *A* at 820 K), similar to the coated LJ (Lennard-Jones) clusters.[30] This indicates that for the embedded particles within a matrix such as Pb in Al, since Pb-Al is an immiscible system, coalescence of the two or more nearby particles can occur after one or several cycles for the solid-liquid transition, as observed experimentally for the Pb-Al samples.[6]

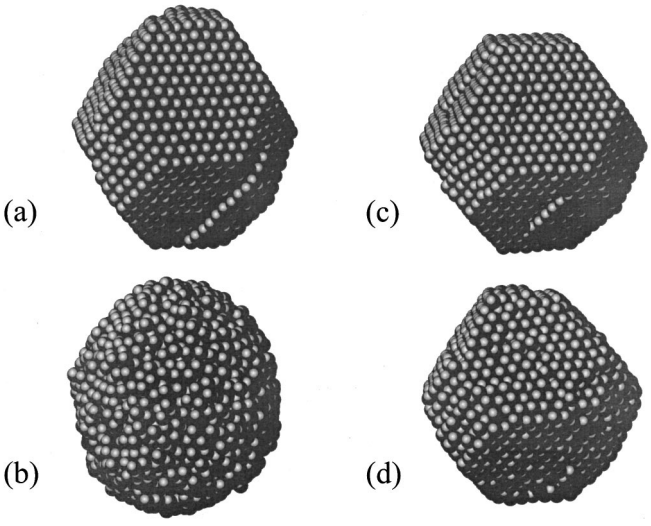

FIG. 6. Snapshots of two coated clusters at different temperatures: (a) cluster *A* at 200 K, (b) cluster *A* at 800 K, (c) cluster *B* at 200 K, and (d) cluster *B* at 625 K.

B. Premelting

The behavior of cluster *B* is quite different from *A*. There is no detectable structural change at low temperatures, indicates that lack of a cube-cube parallel relationship between Pb core and the Al matrix makes it rather difficult to form an effective semicoherent interface. This can be reflected by examining the cross section plot of the cluster at two different temperatures as show in Fig. 5(b). After low temperature relaxation of cluster *B* (the relaxation process also generates some dislocations in the outer Al shells), some point defects (vacancies) at the interfaces of Al and Pb can be redistributed. Hence, the core cluster appeared to be much less bounded by the Al coating, and the energy difference (0.002 a.u. or 0.054 eV) between the two clusters is large, clearly indicates that *B* is less stable than *A*. Heterogeneous nucleation sites can thus be formed at the Al-Pb interface or even inside the Pb core of cluster *B*, which leads to the premelting of the core at about 500 K, or 110 K below the equilibrium melting point for bulk Pb.

However, contrary to the case of cluster *A*, the melting of Pb cluster does not induce a combined melting of Al coating. Instead, the energy of Al atoms in cluster *B* becomes lower and almost identical to that of cluster *A*, as shown in Fig. 4(b). This indicates that the Al coating can be relaxed to a more stable state after the melting of Pb core. The whole cluster will melt not too far below 750 K because an Al cluster with a melted core is much unstable than a perfect cluster of same size. Some flat facets also appeared for the liquid Pb cluster at high temperatures [Fig. 5(b)].

IV. DISCUSSION

The change of the Gibbs free-energy ΔG for melting of embedded spherical particles is given as[45,46]

$$\Delta G = \frac{4}{3}\pi r^3\left(\frac{L}{T_0}(T_0 - T) + \Delta E\right) + 4\pi r^2(\gamma_{\mathrm{LM}} - \gamma_{\mathrm{SM}}), \tag{3}$$

where r is the radius of the particle, L is the latent heat of fusion per unit volume, and γ_{LM} and γ_{SM} are liquid and solid particle-matrix interfacial energies, respectively. ΔE is the strain energy per unit volume resulting from the difference between the coefficients of thermal expansion and volume change. For particles being well confined by the matrix, ΔE can be calculated according to the relation suggested by Allen *et al.*[47] Based on $\partial G/\partial R = 0$, a relationship between melting point and critical radius R can be obtained as

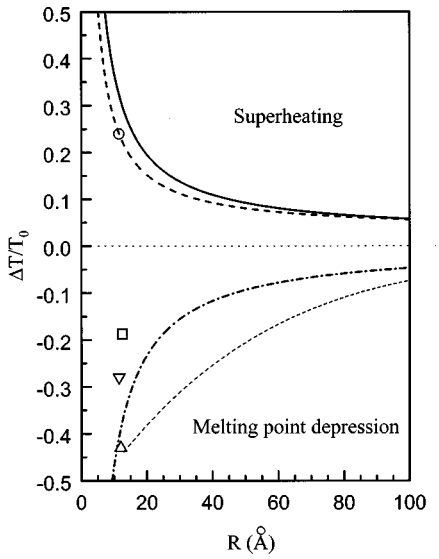

FIG. 7. The degree of superheating or melting point depression of Pb clusters. For MD simulated clusters, the circle, square, down triangle, and up triangle represent, respectively, the Al coated Pb^{201} cluster, Al coated Pb^{249} cluster, Pb^{201} free cluster, and Pb^{249} free cluster. The full line is predicted using Eq. (5) with $\gamma_{LS}=0.047\ \mathrm{Jm}^{-2}$ for Pb, the dashed line is fitted from experimental data for Pb inclusions of Gråbæk *et al.* (Ref. 6), the dot-dashed line is fitted from the experimental data for ball-milled Pb particle embedded in Al matrix of Sheng (Ref. 48), and the short-dashed line is fitted from experimental data for free Pb clusters of Ben David *et al.* (Ref. 49).

$$\frac{T_m(R)-T_0}{T_0}=\frac{1}{L}\left[\Delta E+\frac{2(\gamma_{\mathrm{LM}}-\gamma_{\mathrm{SM}})}{R}\right]. \tag{4}$$

For free clusters, the matrix can be viewed as the vapor phase, and $\Delta E=0$, the relation can be changed to

$$\frac{T_0-T_m(R)}{T_0}=-\frac{2(\gamma_{\mathrm{LV}}-\gamma_{\mathrm{SV}})}{LR}, \tag{5}$$

where γ_{SV} and γ_{SL} represent the solid-vapor and solid-liquid interfacial energies, respectively. Such a formula is similar to Eq. (1). It can be used in interpreting the melting point depressions for free clusters because γ_{SV} is quite larger than γ_{SL} for most metals.

If both the matrix and the embedded cluster consist of the same element, i.e., for a pure substance, Eq. (4) can be converted into

$$\frac{T_m(R)-T_0}{T_0}=\frac{1}{L}\left[\Delta E+\frac{2\gamma_{\mathrm{LS}}}{R}\right]. \tag{6}$$

This relation is just the same one as predicted using the homogeneous nucleation theory for a metastable superheating of an infinite surface-free single crystal.[35]

We use Eq. (4) in fitting the experimentally measured melting point of the Pb inclusions in Al matrix which can exhibit either melting point elevation or depression (see Fig. 7). For the case of superheating, the fitted curve is found to be close but under the one predicted using Eq. (6) with the γ_{SL} being 0.048 Jm^{-2} (γ_{SL} for Pb varies from 0.03–0.07 Jm^{-2} as reported in literature, here we have used a mean value, which is close to 0.046 Jm^{-2} as used in a recent paper[48]). The fitted interfacial energy difference $\gamma_{LM}-\gamma_{SM}$ is 0.038 $\mathrm{J/m}^{-2}$, smaller than γ_{SL} for Pb. This occurs because the observed Pb-Al interface is semicoherent. For In particles embedded inside the Al matrix, the measured value of $\gamma_{LM}-\gamma_{SM}$ is 0.0267 Jm^{-2} according to Zhang and Cantor,[43] very close to the solid-liquid interface energy of pure In metal, i.e., 0.03 Jm^{-2}, indicates that a better semicoherent condition than Pb-Al may exist for In-Al. The superheating of our MD simulated Pb^{201} cluster is 140 K, or $0.23T_0$, very close to the curve fitted from experimental data.

If no semicoherent interface exists, such as in the ball-milled samples, the $\gamma_{LM}-\gamma_{SM}$ value will be negative, and this can result in the melting point depression. Also in using Eq. (4), we have fitted the melting points for the ball-milled Pb inclusions in Al matrix[49] but assuming that ΔE is zero. This curve is plotted in Fig. 7 together with the curve fitted for the measured melting points of free lead particles.[50] The two curves show a large discrepancy for small particles less than 10 nm, suggesting that the surface energies of the balled-milled Pb inclusions is quite different from that of the free particles. Our simulated Pb^{249} cluster provides a direct verification for this point. As shown in Fig. 7, the Al coating may elevate the melting point of the cluster significantly, however, the Pb-Al interface is incoherent and shows a negative interfacial energy difference, the melting point for the cluster cannot exceed the equilibrium melting point of the bulk solid.

The above analysis also suggests that the melting mechanisms of the clusters with different surface/interface may be two folds. On one hand, for embedded clusters with coherent or semicoherent interface with the matrix, the melting of the system can be viewed as a homogeneous process, where each cluster acts as a single nucleate. The melting starts from the inside of the cluster rather than at its surface. Since interface energy difference before and after melting is positive, the embedded cluster can be superheated according to Eq. (4). On the other hand, if the interface is incoherent, a negative interface energy difference may be resulted, and this will lead a melting point depression. Such an interface acts as a heterogeneous nucleation site as the role of the surfaces of free particles. The melting behaviors of our simulated Pb clusters with different Al coatings are consistent with the scenario of homogeneous or heterogeneous nucleation mechanism. We also noted that both melting point elevation and depression have the same thermodynamic origin, hence, the superheating of cluster *A* does not mean that the cluster is in a metastable superheating state.

V. CONCLUDING REMARKS

Different melting behaviors have been studied for Pb clusters without free surfaces in using molecular dynamics and the Sutton-Chen many-body potentials. For these clusters, the melting temperature can be either elevated or depressed, which will depend on whether the heterogeneous nucleation sites at the surfaces can be effectively eliminated or not. If the core Pb cluster is in a cube-cube relationship with the Al matrix, semicoherent interfaces can be formed combined with the generation of dislocations and the cluster can be superheated, followed by simultaneous melting of the

whole cluster on elevated temperatures. While without a cube-cube relationship, no semicoherent interfaces can be formed and the core cluster will premelt, and the crystalline lattices of Al coating does not destroyed by the melting of the core. The melting points can be predicted based on thermodynamic relations where the interfacial energy difference acts as a crucial role. A positive energy difference between liquid-matrix and solid-matrix interface will lead to a considerable superheating for the cluster. In contrary, a negative one will lead to a melting point depression. Melting behaviors of the simulated clusters are consistent with the homogeneous or inhomogeneous melting mechanism.

ACKNOWLEDGMENTS

It is the author's pleasure to thank J. Q. Broughton for useful suggestions. Financial support from Chinese Academy of Sciences and National Science Foundation of China (Grant Nos. 59625101, 59801011, and 59841004) is gratefully acknowledged.

APPENDIX A: INTERATOMIC POTENTIALS FOR Al-Pb BINARY SYSTEM

In the Sutton-Chen ''glue'' scheme, the total energy for pure metals is expressed as a summation over atomic positions:[38]

$$E_{\mathrm{tot}}=\varepsilon\left[\frac{1}{2}\sum_{i\neq j}V(r_{ij})-c\sum_{i}\rho_i^{1/2}\right],$$

$$V(r)=\left(\frac{a}{r}\right)^{n},$$

$$\rho_i=\sum_{j\neq i}\left(\frac{a}{r_{ij}}\right)^{m}, \tag{A1}$$

where c is a positive dimensionless parameter, ε is a parameter with the dimensions of energy, a is a parameter with the dimensions of length, ρ_i is the local atomic density around atom i, and m and n are positive integers.[38,51]

The generalization of Eq. (A1) to describe binary A-B alloys is straightforward by assuming that the interactions between like pairs are the same as in the pure metals. The energy contributions to ith atom (A or B) from unlike atoms (B or A) can be given as

$$E_i^{AB}=\frac{1}{2}\varepsilon^{AB}\sum_{i\neq j}V^{AB}(r_{ij})+\varepsilon^{AA}c^{AA}(\rho_i)^{1/2}$$

or

$$E_i^{BA}=\frac{1}{2}\varepsilon^{BA}\sum_{i\neq j}V^{BA}(r_{ij})+\varepsilon^{BB}c^{BB}(\rho_i)^{1/2}, \tag{A2}$$

where

$$V^{AB}(r)=V^{BA}(r)=\left(\frac{a^{AB}}{r}\right)^{n^{AB}} \tag{A3}$$

and

TABLE I. Parameters for Sutton-Chen potentials used for Al-Pb (fitted from room temperature properties).

	a (Å)	ε (10^{-3} eV)	c	m	n	δ
Pb-Pb	4.95	5.5765	45.7811	7	10	
Al-Al	4.05	9.1435	52.2066	5	9	
Pb-Al	4.48	7.1406		6	10	0.5

$$\rho_i=\sum_{j\neq i}\left(\frac{a^{AB}}{r_{ij}}\right)^{m^{AB}}=\sum_{j\neq i}\phi^{AB}(r_{ij}), \tag{A4}$$

with only four parameters ε^{AB}, a^{AB}, m^{AB}, and n^{AB} left to be determined additionally. In the Sutton-Chen's scheme, these parameters are given empirically by expressing the functions V^{AB} and ϕ^{AB} as

$$V^{AB}=(V^{AA}V^{BB})^{1/2} \tag{A5}$$

and

$$\phi^{AB}=(\phi^{AA}\phi^{BB})^{1/2}, \tag{A6}$$

which lead to

$$m^{AB}=\frac{1}{2}(m^{AA}+m^{BB}),$$

$$n^{AB}=\frac{1}{2}(n^{AA}+n^{BB}),$$

$$a^{AB}=(a^{AA}a^{BB})^{1/2},$$

$$\varepsilon^{AB}=\varepsilon^{BA}=(\varepsilon^{AA}\varepsilon^{BB})^{1/2}. \tag{A7}$$

Thus, all parameters in Sutton-Chen's formula for binary alloys can be obtained from the parameters for the pure A and B metals. However, the Al-Pb alloy is a typical immiscible alloy system as shown in the equilibrium phase diagram, the potential constructed according to Eq. (A7) may be inadequate to be used for this alloy. Provided that Eq. (A7) is purely empirical, we can readjust m^{AB} or n^{AB} or both of them in order to obtain a good description of the phase separating or compound forming tendency by introducing a simple modification scheme. For Al-Pb system, this can be realized by making n^{AB} slight larger than the mean value of n^{A} and n^{B}, i.e.,

$$n^{AB}=\frac{1}{2}(n^{AA}+n^{BB})+\delta, \tag{A8}$$

where δ is set to be 0.5 in our calculations. Such a procedure imposes the separation tendency between Al and Pb atoms by strengthening their repulsive interactions. The mixing enthalpy is predicted to be positive, i.e., $\Delta H=0.625k_BT$ (at $T=1200\,\mathrm{K}$ and zero pressure), in good agreement with the value given by Singh and Sommer,[52] i.e., $0.847k_BT$ for the liquid $Al_{0.5}Pb_{0.5}$ alloy. All parameters used for Al-Pb Sutton-Chen scheme have been listed in Table I.

Another point to be considered is the truncations of the potentials in MD simulations. Considering that the Sutton-Chen potential is long-ranged, our approach in truncation is to retain the full Sutton-Chen force within the range of $0 < r \leqslant 2.3a_0$, but to use a modified force in the range $2.3a_0 < r \leqslant 2.5a_0$ (a_0, the lattice parameter at 0 K). Here, we used a similar procedure given by Broughton for a typical LJ potential in investigation of the bulk solid and clusters.[15,30]

*Electronic address: zhjin@imr.ac.cn

[1] *Physics and Chemistry of Finite Systems: from Clusters to Crystals*, edited by P. Jena, S. N. Khanna, and B. K. Rao (Kluwer, Dordrecht, 1992).

[2] J.-P. Borel, Surf. Sci. **106**, 1 (1981).

[3] P. Pawlow, Z. Phys. Chem., Stoechiom. Verwandtschaftsl. **65**, 1 (1909); **65**, 545 (1909).

[4] F. Ercolessi, W. Andreoni, and E. Tosatti, Phys. Rev. Lett. **66**, 911 (1991).

[5] J. Däges, H. Gleiter, and J. H. Perepezko, Phys. Lett. A **119**, 79 (1986).

[6] L. Gråbæk, J. Bohr, H. H. Andersen, A. Johansen, E. Johnson, L. Sarholt-Kristensen, and I. K. Robinson, Phys. Rev. B **45**, 2628 (1992).

[7] E. Johnson, K. Hjemsted, B. Schmidt, K. K. Bourdelle, A. Johansen, H. H. Andersen, in *Phase Formation and Modification by Beam-Solid Interactions*, edited by G. S. Was, L. E. Rehn, and D. Follstaedt, MRS Symposia Proceedings No. 235 (Materials Research Society, Pittsburgh, 1992), p. 485.

[8] K. K. Bourdelle, A. Johansen, E. Johnson, L. Sarholt-Kristensen, S. Steenstrup, and L. Yu, Nucl. Instrum. Methods Phys. Res. B **80/81**, 317 (1993); H. H. Andersen and E. Johnson, *ibid.* **106**, 480 (1995).

[9] C. J. Rossouw and S. E. Donnelly, Phys. Rev. Lett. **55**, 2960 (1985).

[10] R. W. Cahn, Nature (London) **323**, 668 (1986).

[11] R. Garrigos, R. Kofman, P. Cheyssac, and M. Y. Perrin, Europhys. Lett. **1**, 355 (1986).

[12] G. D. T. Spiller, Philos. Mag. A **46**, 535 (1982).

[13] H. W. Sheng, G. Ren, L. M. Peng, Z. Q. Hu, and K. Lu, Philos. Mag. Lett. **73**, 179 (1996).

[14] S. Q. Xiao, E. Johnson, S. Hinderberger, A. Johansen, K. K. Bourdelle, and U. Dahmen, J. Microsc. **180**, 61 (1995).

[15] J. Q. Broughton and G. H. Gilmer, J. Chem. Phys. **79**, 5095 (1983); Acta Metall. **31**, 845 (1983).

[16] H. S. Lim, C. K. Ong, and F. Ercolessi, Z. Phys. D **26**, S45 (1993); Surf. Sci. **269/270**, 1109 (1992); Comput. Mater. Sci. **2**, 495 (1994); Phys. Rev. B **50**, 17 507 (1994).

[17] G. Bilalbegović and E. Tosatti, Phys. Rev. B **48**, 11 240 (1993).

[18] O. Gülseren, F. Ercolessi, and E. Tosatti, Phys. Rev. B **51**, 7377 (1995).

[19] F. Ercolessi, S. Iarlori, O. Tomagnini, E. Tosatti, and X. J. Chen, Surf. Sci. **251/252**, 645 (1991).

[20] C. Rey, L. J. Gallego, J. García-Rodeja, J. A. Alonso, and M. P. Iñiguez, Phys. Rev. B **48**, 8253 (1993).

[21] C. L. Cleveland and Uzi Landman, J. Chem. Phys. **94**, 7376 (1991).

[22] J. M. Montejano-Carrizales, M. P. Iñiguez, and J. A. Alonso, J. Cluster Sci. **5**, 287 (1994).

[23] E. T. Chen, R. N. Barnett, and Uzi Landman, Phys. Rev. B **41**, 439 (1990).

[24] D. Wolf, P. R. Okamoto, S. Yip, J. F. Lutsko, and M. Kluge, J. Mater. Res. **5**, 286 (1990).

[25] P. Stoltze, J. K. Nørskov, and U. Landman, Phys. Rev. Lett. **61**, 440 (1988).

[26] P. Stoltze, J. Chem. Phys. **92**, 6306 (1990).

[27] K. W. Jacobsen, O. H. Nielsen, and O. B. Christensen, in *Computations for the Nano-Scale*, edited by P. E. Blöchl *et al.* (Kluwer, Dordrecht, 1993), p. 115.

[28] J. Andrew Combs, Phys. Rev. Lett. **61**, 714 (1988).

[29] L. L. Boyer, Phys. Rev. B **53**, 3145 (1996).

[30] J. Q. Broughton, Phys. Rev. Lett. **67**, 2990 (1991); Phys. Rev. B **46**, 2523 (1992).

[31] D. G. Grier, Nature (London) **379**, 773 (1996).

[32] A. R. Ubbelohde, *Melting and Crystal Structure* (Clarendon, Oxford, 1965).

[33] S. R. Phillpot, J. F. Lutsko, D. Wolf, and S. Yip, Phys. Rev. B **40**, 2831 (1989).

[34] J. F. Lutsko, D. Wolf, S. R. Phillpot, and S. Yip, Phys. Rev. B **40**, 2841 (1989).

[35] Z. H. Jin and K. Lu, Philos. Mag. Lett. **78**, 29 (1998).

[36] K. Lu and Y. Li, Phys. Rev. Lett. **80**, 4474 (1998).

[37] Z. H. Jin and K. Lu (unpublished).

[38] A. P. Sutton and J. Chen, Philos. Mag. Lett. **61**, 139 (1991).

[39] F. Ercolessi, O. Tomagnini, S. Iarlori, and E. Tosatti, in *Nanosources and Manipulation of Atoms Under High Fields and Temperatures: Applications*, Vol. 235 of *NATO Advanced Study Institute, Series E: Applied Science*, edited by Vu Thien Binh, N. Garcia, and K. Dransfeld (Kluwer, Dordrecht, 1993), p. 185.

[40] Superheating of Pb(111) and Al(111) above the bulk melting temperature have been observed experimentally and studied theoretically. See, e.g., J. W. Herman and H. E. Elsayed-Ali, Phys. Rev. Lett. **69**, 1228 (1992); F. D. Di Tolla, F. Ercolessi, and E. Tosatti, *ibid.* **74**, 3201 (1995); G. Bilalbegović, Phys. Rev. B **55**, 16 450 (1997).

[41] M. Schmidt, R. Kusche, B. Von Issendorff, and H. Haberland, Nature (London) **393**, 238 (1998).

[42] Relations of mean atomic volumes (in atomic units) with temperature fitted for Pb and Al from the constant pressure MD in using the SC potentials:

$$\Omega_{\mathrm{Pb}}(T) = 204.4193 + 2.8320\times10^{-2}T - 1.4075\times10^{-5}T^2 + 3.1120\times10^{-8}T^3,$$

$$\Omega_{\mathrm{Al}}(T) = 112.1709 + 9.4094\times10^{-3}T + 1.3194\times10^{-7}T^2 + 1.7773\times10^{-9}T^3.$$

[43] D. L. Zhang and B. Cantor, Philos. Mag. A **62**, 557 (1990); Acta Metall. Mater. **39**, 1595 (1991).

[44] L. J. Lewis, P. Jensen, and J.-L. Barrat, Phys. Rev. B **56**, 2248 (1997).

[45] J. H. Hollomon and D. Turnbull, Prog. Met. Phys. **4**, 333 (1953); B. Chalmers, *Principles of Solidification* (Wiley, New York, 1964).

[46] D. A. Porter and K. E. Easterling, *Phase Transformation in Metals and Alloys* (Van Nostrand Reinhold, New York, 1988).

[47] G. L. Allen, W. W. Gile, and W. A. Jesser, Acta Metall. **28**, 1695 (1980).

[48] K. F. Peters, J. B. Cohen, and Y.-W. Chung, Phys. Rev. B **57**,

13 430 (1998).
[49] H. W. Sheng, Ph.D. thesis, Institute of Metal Research, Chinese Academy of Sciences, 1997.
[50] T. Ben David, Y. Lereah, G. Deutscher, R. Kofman, and P. Cheyssac, Philos. Mag. A **71**, 1135 (1995).
[51] H. Rafii-Tabar and A. P. Sutton, Philos. Mag. Lett. **63**, 217 (1991).
[52] R. N. Singh and F. Sommer, Rep. Prog. Phys. **60**, 57 (1997).